Enhancement of LiFePO4 (LFP) Electrochemical PerformanceTthrough the Insertion of Coconut Shell Derived rGO – Like Carbon as Cathode of Li-ion Battery

Eka Suarso (eka.suarso1979@gmail.com)
Institut Teknologi Sepuluh Nopember https://orcid.org/0000-0001-9867-7578

Firsta Agung Setyawan
Institut Teknologi Sepuluh Nopember

Achmad Subhan
Lembaga Ilmu Pengetahuan Indonesia

Muhammad Mahyiddin Ramli
University Malaysia Perlis School of Microelectronic Engineering: Universiti Malaysia Perlis Sekolah Kejuruteraan Mikroelektronik

Nur Syakimah Ismail
University Malaysia Perlis School of Microelectronic Engineering: Universiti Malaysia Perlis Sekolah Kejuruteraan Mikroelektronik

Mochamad Zainuri
Institut Teknologi Sepuluh Nopember

Zaenal Arifin
Institut Teknologi Sepuluh Nopember

Darminto Darminto
Institut Teknologi Sepuluh Nopember

Research Article

Keywords: reduced graphene oxide (rGO), LFP (LiFePO4), LFP/rGO, nanocomposites, and mechanical ultracentrifugation method.

Posted Date: April 26th, 2021

DOI: https://doi.org/10.21203/rs.3.rs-298403/v1

Abstract

In this study, an rGO – like carbon (C) compound was synthesized from coconut shell (biomass), and inserted into $LiFePO_4$ (LFP), as Li-ion battery cathode. Thus, an LFP/C nanocomposite was successfully fabricated using a combination of the sol-gel technique and mechanical ultracentrifugation. $LiFePO_4$ precursors were prepared from commercial starting materials, using the sol-gel technique, and the composites' carbon weight content was varied between 15% and 30%. Subsequently, the microstructural characteristics and electrochemical properties as cathode for Li-ion batteries were measured. In addition to exhibiting higher electrical conductivity, the synthesized LFP/C nanocomposite showed higher capacity and better cycle capability. Also, the nanocomposite cathode showed a specific capacity of 128 $mAhg^{-1}$ in the first cycle, and a retention capacity of 75% after 10 cycles, at room temperature and a rate of 0.1 C. The enhanced electrical conductivity and electrochemical performance of the samples prepared are believed to be due to three-dimensional conduction network formed by the rGO like carbon sheets, as observed by electron microscopy.

1. Introduction

Lithium iron phosphate (LFP) was first reported in 1997, by Goodenough *et al.*, as a promising cathode material for rechargeable Li-ion batteries, and has long been studied intensively afterwards [1,2]. This is due the easily obtainable, non-toxic, environmentally friendly and cheaply manufactured constituent materials [2–4]. In addition, LFP with olivine structure ($LiFePO_4$) shows a high theoretical capacity (170 $mAhg^{-1}$), suitable operating voltage (3.5V vs Li^+/Li), long life, and high thermal stability [3,4]. However, low intrinsic electronic conductivity and slow diffusion rate of lithium ions have limited the application in Li-ion batteries, particularly at low temperatures and high current densities [3,5]. Therefore, a combination of carbon bridging and particle size reduction is one of the most effective strategies to overcome this problem [2,5,6]. This carbon bridging effort aims to inhibit crystal growth [7], blocking particle agglomeration [8], strengthen contact inter-particles [9], and shorten the lithium ion diffusion pathways [10,11], while the presence of a carbon layer prevents Fe^{2+} oxidization to Fe^{3+}, thus, the material's purity is guaranteed [11].

Graphene sheets, including reduced graphene oxide (rGO), are of particular interest among the various activated carbon materials available, due to high electronic conductivity, wide surface area, structural flexibility and unique characteristics of a single atomic thick layer [12–14]. The preparation of LFP/rGO nanocomposites does not only tend to improve the cathode material's conductivity, but also shortens the lithium ions' diffusion path, while increasing the lithium ion diffusion rate, thus, improving the material's electrochemical performance [15]. During the last decade, research on bridging LFP cathode material with graphene or rGO in composite form were conducted [3,12]. Shang *et al.*, synthesized a LFP/graphene composite by the liquid phase method, and the results showed a initial specific discharge capacity of 160 $mAhg^{-1}$ at 0.1 C [16]. Meanwhile, Yuan *et al.*, synthesized a $LiFePO_4$/rGO composite through a simple solid phase combined with a carbothermal reduction method, and the results show a first special

discharge capacity of 151.5 $mAhg^{-1}$ at 0.1 C, and 149.2 $mAhg^{-1}$ after 50 cycles, with a coulombic efficiency of 98.5% [17]. Furthermore, Dhindsa *et al.*, synthesized $LiFePO_4$/graphene nanocomposites using the sol-gel method, and the constant current test results showed $LiFePO_4$/G composite had a higher initial discharge capacity at a 0.1C current density, compared to pure $LiFePO_4$ [18]. Similarly, Yuan et al., successfully prepared rGO composites based on $LiFePO_4$ using the hydrothermal method [19], almost all the results indicated better electrochemical performance and stability in the composites. LFP/graphene composites have also been successfully prepared through in-situ solvothermal methods [20,21], solid state reaction [22,23], and co-precipitation method [24]. Generally, the composites produced from these various synthesis methods have significantly improved the $LiFePO_4$ electrode's electrochemical performance [19]. In terms of simplicity, manufacturing $LiFePO_4$ nanocomposites to control $LiFePO_4$'s morphology is preferable because nanocomposites are made by simply mixing components and the conductivity is controlled by careful components selection [23,25,26].

Nano-structured $LiFePO_4$ particles and rGO potentials are believed to be suitable candidates for further developing cathode materials for lithium-ion batteries. Therefore, this study aims to synthesize and characterize the LFP cathode material, using the sol-gel method, as well as to identify and analyse the effect of carbon compounds insertion on the cathode materials' electrochemical performance. In this study, an old coconut shell (biomass) was used to prepare an rGO – like carbon, as a "green" (sustainable) compound, for use in battery technology.

2. Method

$LiFePO_4$ nanoparticles were prepared by sol-gel method using Li_2CO_3, $FeCl_2.4H_2O$, and $NH_4H_2PO_4$ powders as precursors. The materials were then mixed and homogenized into a solution, using a magnetic stirrer. Subsequently, the resulting sol solution was slowly dripped with NH_4OH until a pH of 7 was obtained, while continuously stirred and heated at 100^oC for 3 hours, to form a gel. This was followed by drying the precursor gel at 120^oC to obtain xerogel and calcination at 700^oC and 750^oC in an argon gas environment, for 10 hours, at 5^oC/second. Meanwhile, the (rGO like) carbon compound was synthesized from old coconut shells, subjected to burning, pulverizing as well as sieving, and the charcoal powder obtained was carbonized in a furnace at 400^oC, for 5 hours. Furthermore, a mechanical and chemical cutting process were carried out for 6 hours to release the bonds between carbon hexagonal strutctures (rGO layers) reduce the particle size.

The $LiFePO_4$ was composited with rGO-like carbon solution, using the mechanical ultracentrifugation method. This was performed by adding the solution to LFP particles and mixing with a buthanol (N-buthanol). The mixture was then dispensed and stirred with a magnetic stirrer at 120^oC for 5 hours. Subsequently, the sample was ultrasonised until the rGO layers was estimated to cover the LPF particles, and subjected to polarization. The LFP/rGO slurry obtained was then centrifuged at 6000 rpm for 40

minutes to form a LFP/rGO nanocomposite structure, and dried at 80^{o}C for 2 hours. This process is an advancement of the previous method [27].

The LFP nanoparticles' crystal structure, phase composition and lattice parameters were examined using the Philips X'Pert MPD X-Ray Diffraction instrument (Multipurpose Diffractometer), and Cu Kα (λ = 1.54060 Å) radiation. Meanwhile the morphology and crystal size were observed by Scanning Electron Microscopy (SEM-EDX, ZEISS).

The $LiFePO_4$-based nanocomposite cathode's electrochemical properties were measured using a CR2016 coin cell, with a lithium metal disc as the counting electrode. Meanwhile, the working electrodes were assembled by pressing a mixture of the synthesized $LiFePO_4$/rGO, polyvinylidene fluoride (PVDF) binder and super-p addictive material, in a 0.5: 0.033: 0.022 weight ratio. The electrolyte was created from 1M $LiPF_6$ dissolved in a mixture of ethylene carbonate (EC) and dimethyl carbonate (DMC) (1: 1: 1, v / v / v) as well as Li-foil and Celgard 2300 microfilm used as a separator and counter electrode. Furthermore, the coin cells were assembled in a glove box filled with high purity Ar gas, while the $LiFePO_4$/rGO electrical conductivity test was conducted with a four-point probe. The galvanostatic charge/discharge is tested in the voltage range 0.5-4.0 V vs Li/Li^+ at various current levels, while electrochemical impedance spectroscopy (EIS) and cyclic voltammetry (CV) were measured above the CHI-660D electrochemical workstation, at 0.1 mVs^{-1} in 0.5-2.1 V vs $Zn°/Zn^{2+}$. Also, EIS measurements were performed over the frequency range 0.01 Hz - 100 kHz at the discharge stage, with 5 mV amplitude.

3. Results And Discussion

Figure 1 shows the X-ray diffraction (XRD) patterns revealed by the two LFP sample structure shapes and phase purities. Based on phase identification from the XRD pattern results, the two LFP sample's crystalinity were analyzed. Both patterns show similar LiFePO4 main diffraction peaks and match the orthorhombic structure as well as Pnma space group. The sharp, narrow diffraction peaks without detectable phase impurities indicate the LFP sample has high crystalinity. For the sample calcined at 750^{o}C, an olivine phase without detectable impurity phases was observed, while the 700^{o}C sample showed a 97% pure olivine phase, and a phase impurity in the form of $FeO_{11}P_4$. The LFP sample calcined at 750^{o}C had a sharper diffraction peak with narrower full width at half maximum (FWHM) and a higher intensity, compared to the 700^{o}C counterpart. According to the peak FWHM, the crystal size of the samples prepared at 700°C and 750°C calculated by the Scherrer equation resulted in 99 nm and 100 nm, respectively.

The LFP/rGO nanocomposite particles' morphological and microstructure are observable with SEM-EDX (Figure 2). Based on the images, LFP particles have spherical lumps and are firmly attached to rGO, resembling a thin flake (Figures 2a and b). LFP's spherical lumps indicate agglomeration, where several particles are joined together to look larger, with a non-homogenous and unevenly distributed grain size in certain places. This agglomeration occurs because the LFP powder, rGO solution, and N-butanol are not

evenly mixed in the slurry-making process, while, the black lumps indicate the cathode sheet has shafts. Figure 2b shows large LFP particles are scattered and firmly attached to each rGO layer side, thus, acting as a “bridge” among the particles surroundings. Lithium ion has a greater diffusion distance between the crystal grain’s boundary and center, due to the larger crystal size. Furthermore, the rGO bridge is quite effective in limiting the LFP’s grain growth and widening the surface area, thus shortening the lithium ion’s diffusion length. Therefore, the close relationship between LFP and rGO nanoparticles encourages maximum efficiency while implementing the framework. Also, the presence of Fe, P, O, and C were confirmed in EDX elemental analysis for the LFP/rGO nanocomposite.

Figure 3 shows the LFP/rGO nanocomposites’ electronic conductivity and stored energy, and these are much higher, compared to pure LFP. Mixing $LiFePO_4$ particles with rGO by mechanical ultrasonification plays a significant role in enhancing the electronic conductivity and stored energy, and these properties increase with increase in rGO percentage. The optimum result of $7.84x10^{-4}$ S/cm was obtained for samples with a mass ratio of 70% LFP and 30% rGO, while the counterparts for pure $LiFePO_4$ (theoretical), and LFP synthesized by the sol-gel method are ~ 10^{-9} S/cm and 2.09 x 10^{-7} S/cm, respectively.

Meanwhile, energy stored from LFP/rGO nanocomposites show a unique phenomenon, and the optimum value of $6.50x10^{-3}$ J was obtained by samples with a mass ratio of 85% LFP and 15% rGO. This explains the addition of rGO bridging LFP particles must be carried out within certain limits, and is reinforced by the LFP/rGO nanocomposite cathode material’s electrochemical properties. A lithium battery’s energy capacity depends on how many lithium ions are stored in the electrode structure, and how much the ions are able to move during charging and discharging, because the amount of electron current stored and distributed is proportional to the amount of lithium ions diffused. Further discussion is to refer to the two samples, for a comparative study.

Figure 4 shows the LFP/rGO nanocomposite’s cyclic voltammogram curve, with the addition of 15% and 30% rGO percentages in the first charge-discharge cycle. Both curves show sharp and symmetric anodic/cathodic peaks, indicating good electrochemical performance due to single electron transfer reaction during the cycle. In addition, both electrodes showed a Fe^{2+}/Fe^{3+} redox peak at a 0.1 mVs^{-1} scan rate. Meanwhile, for LFP/rGO nanocomposites with a 85% - 15% mass ratio, the anodic peak was located at 3.46V, and this corresponds to the oxidation of Fe^{2+} to Fe^{3+}, while the cathodic peak at 3.30V corresponds to the reduction of Fe^{3+} to Fe^{2+}, with a 0.16V potential interval between the two redox peaks. The anodic and cathodic peaks voltage difference within the same cycle correlates with the redox reaction’s polarization and inverse, and this indicates the battery material’s reversibility. A reduction in voltage difference lowers the polarization and increases the battery material’s reversibility, resulting in greater cycle stability. This is consistent with the charge-discharge graph and accelerates the Li^+ ions’ diffusion rate. The observed separation between the oxidation and reduction peaks is often used to distinguish electrochemical reversibility from electrode materials, with larger separations indicating lower reversibility. This narrow separation from the redox peak implies the LFP/rGO nanocomposite has excellent electrochemical kinetics.

Figure 5 shows the Nyquist plot, derived from the electrochemical impedance spectroscopies (EIS) of both LFP/rGO nanocomposite samples, measured to further prove the rGO thin-layers in LFP/rGO nanocomposites increase the material's the electronic conductivity. According to the image, the nyquist plots obtained are in the form of semicircles and slopes. The semicircle pattern in moderate frequency region shows the lithium ion's charge transfer process on the LFP/rGO and electrolyte surfaces. Meanwhile, the straight line pattern represents the lithium ion diffusion process into the electrode bulk material, commonly known as Warburg diffusion. This pattern shows the electrodes are capable of storing lithium ions, and are therefore suitable for use in lithium-ion batteries. The charge-transfer resistance width also determines the battery's electrical conductivity of the battery. An increase in pattern narrowness leads to an increase in electrical conductivity.

A comparison of the EIS profile semicircle diameters shows the LFP/rGO nanocomposite cathode with a weight ratio of 70% - 30% (∼400 ohm) has a much smaller charge-transfer resistance, compared to the counterpart with a ratio of 85% - 15% (∼450 ohm). This much smaller solid-electrolyte interface resistance ought to be due to the rGO layers' presence in the LFP/rGO nanocomposite, with a much better electronic conductivity.

The galvanostatic charge-discharge was measured with lithium cells at a current density of 0.1C (1C = 170 mAg^{-1}), to evaluate the LFP/rGO nanocomposite's electrochemical properties. The results obtained were as a graph of the relationship between the voltage and the charge-discharge capacity, provided with a constant current and a cut-off voltage of 2.5 - 4.2 volts, during the analysis. Furthermore, the cut off voltage is the initial voltage before treatment (charging and discharging). During charging, lithium ions move from anode to cathode until a maximum voltage of 4.2 volts is reached. Subsequently, the ions move from cathode to anode until a minimum voltage of 2.5 volts is reached (discharging). Figure 6 shows the initial cycle profile of the LFP/rGO nanocomposite electrode with a mass ratio of 85% -15% and 70% -30%, at room temperature. According to the image, the first cycle's charge profile shows a stable voltage at 3.5V (versus Li^+/Li), and this must correspond to the redox pair Fe^{2+}/Fe^{3+}. The discharge profile from the first cycle shows a stable voltage at 3.3V (versus Li^+/Li), with a very small separation (0.2V) being stable at the charge profile. In the first cycle, the specific discharge capacity is 128 $mAhg^{-1}$, and this is about 75% of $LiFePO_4$'s theoretical specific capacity. This excellent electrochemical performance is attributed to the large specific surface area and a wide bridging layer, ensuring electrons pass through each LiFePO4 particle, shortening electronic transport pathways, and reducing interface resistance. The lithium ions easily intercalate into the $LiFePO_4$ framework through the rGO layer, and this in turn avoids particle structure collapse during the charge shedding. Therefore, the LFP/rGO nanocomposite structure endures high current density charge/discharge.

4. Conclusion

LFP/rGO nanocomposites were successfully synthesized by combining the sol-gel route and mechanical ultracentrifugation techniques as an alternative to lithium ion battery cathode materials. The content of

rGO prepared from biomass (old coconut shell) was varied between 15% and 30%, and the results showed higher electrical conductivity and capacity, as well as better cycle performance in LFP/rGO nanocomposites, compared to pure LiFePO4 particles. In addition, the nanocomposite cathode showed a specific capacity of 128 $mAhg^{-1}$ in the first cycle and a retention capacity of 75% after 10 cycles, at room temperature and speed of 0.1 C. The improved electrical conductivity and electrochemical performance of the prepared samples are believed to be due to a three-dimensional conduction network provided by rGO-like carbon sheets, as observed by electron microscopy. Also, the LFP particles are scattered and firmly attached to each rGO layer side, thus, acting as a "bridge" among the LFP particles surroundings. The lithium ion has a greater diffusion distance between the crystal grain's boundary and center, due to larger crystal size, and the rGO bridge is quite effective in limiting LFP grain growth as well as widening the surface area, thus shortening the lithium ions diffusion rate. Therefore, the close relationship between LFP and rGO nanoparticles drives maximum efficiency in the implementation.

Declarations

Acknowledgments

The author would like to thank the Indonesian Endowment Fund for Education (LPDP) from the Indonesian Ministry of Finance for a full-ride scholarships through the BUDI-DN Doctorate program. One the author (ES) would like to thank the Laboratory of Microelectronics and Laboratory of Institute of Nanoelectronics Engineering, University of Malaysia Perlis.

CONFLICT OF INTEREST STATEMENT

We are the authors declare that we do not have a conflict of interest.

References

1. A.K. Padhi, K.S. Nanjundaswamy, J.B. Goodenough, J. Electrochem. Soc. **144**, 1188 (1997)
2. N.A. Hamid, S. Wennig, S. Hardt, A. Heinzel, C. Schulz, H. Wiggers, J. Power Sources **216**, 76 (2012)
3. C. Gong, Z. Xue, S. Wen, Y. Ye, X. Xie, J. Power Sources **318**, 93 (2016)
4. Z. Yu, L. Jiang, Solid State Ion. **325**, 12 (2018)
5. A. Eftekhari, J. Power Sources 17 (2017)
6. J. Ma, B. Li, H. Du, C. Xu, F. Kang, J. Solid State Electrochem. **16**, 1353 (2012)
7. Z. Li, J. Mater. Sci. 8 (n.d.)
8. L.N. Sun, Z.Y. Yuan, Y.F. Xue, W.L. Hong, X.Z. Ren, and P. X. Zhang, 900, 4 (n.d.)
9. Y. Liu, C. Cao, J. Li, Electrochim. Acta **55**, 3921 (2010)
10. H. Gong, H. Xue, T. Wang, J. He, J. Power Sources 8 (2016)
11. J. Wang, Ceram. Int. 7 (2014)

12. S.N. Alam, N. Sharma, L. Kumar, Graphene **06**, 1 (2017)
13. P. Russo, A. Hu, G. Compagnini, 14 (n.d.)
14. H. Bi, F. Huang, Y. Tang, Z. Liu, T. Lin, J. Chen, W. Zhao, Electrochim. Acta **88**, 414 (2013)
15. A.V. Murugan, T. Muraliganth, A. Manthiram, J. Phys. Chem. C **112**, 14665 (2008)
16. W. Shang, L. Kong, X. Ji, Solid State Sci. **38**, 79 (2014)
17. Z. Yuan, Y. Xue, L. Sun, Y. Li, H. Mi, L. Deng, W. Hong, X. Ren, P. Zhang, Ferroelectrics **528**, 1 (2018)
18. K.S. Dhindsa, B.P. Mandal, K. Bazzi, M.W. Lin, M. Nazri, G.A. Nazri, V.M. Naik, V.K. Garg, A.C. Oliveira, P. Vaishnava, R. Naik, Z.X. Zhou, Solid State Ion. **253**, 94 (2013)
19. G. Yuan, J. Bai, T.N.L. Doan, P. Chen, Mater. Lett. **158**, 248 (2015)
20. R. Wang, C. Xu, J. Sun, L. Gao, J. Jin, C. Lin, Mater. Lett. **112**, 207 (2013)
21. C. Su, X. Bu, L. Xu, J. Liu, C. Zhang, Electrochim. Acta **64**, 190 (2012)
22. X. Lei, H. Zhang, Y. Chen, W. Wang, Y. Ye, C. Zheng, P. Deng, Z. Shi, J. Alloys Compd. **626**, 280 (2015)
23. Z. Tian, S. Liu, F. Ye, S. Yao, Z. Zhou, S. Wang, Appl. Surf. Sci. **305**, 427 (2014)
24. Y. Ding, Y. Jiang, F. Xu, J. Yin, H. Ren, Q. Zhuo, Z. Long, P. Zhang, Electrochem. Commun. **12**, 10 (2010)
25. W. Song, J. Liu, L. You, S. Wang, Q. Zhou, Y. Gao, R. Yin, W. Xu, Z. Guo, J. Power Sources **419**, 192 (2019)
26. S.H. Ha, Y.J. Lee, Chem Eur J 8 (2014)
27. E. Suarso, A.Z. Laila, F.A. Setyawan, M. Zainuri, Z. Arifin, Darminto, Mater. Sci. Forum **966**, 386 (2019)

Figures

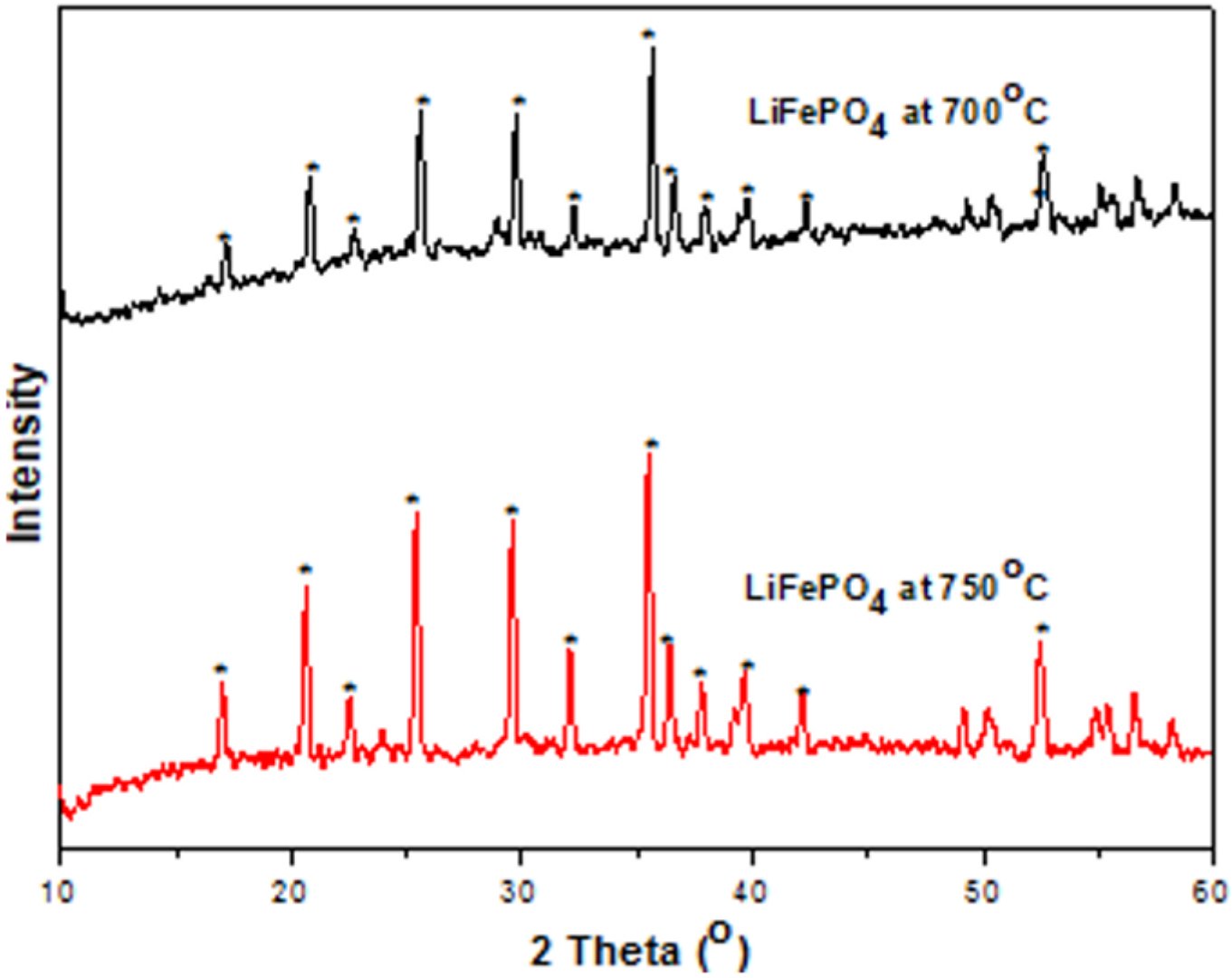

Figure 1

XRD patterns of LFP prepared at temperatures of 700°C and 750°C

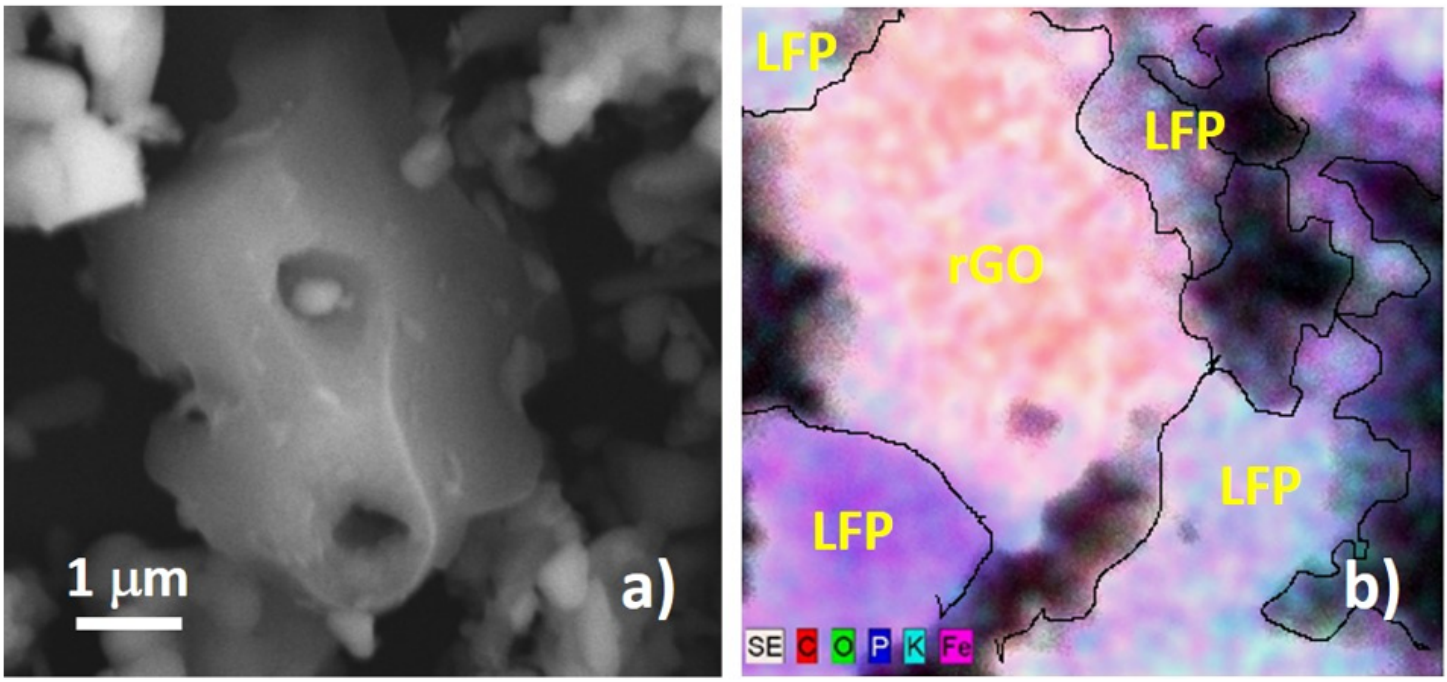

Figure 2

Images of (a) SEM and (b) EDX for nanocomposite LFP/rGO

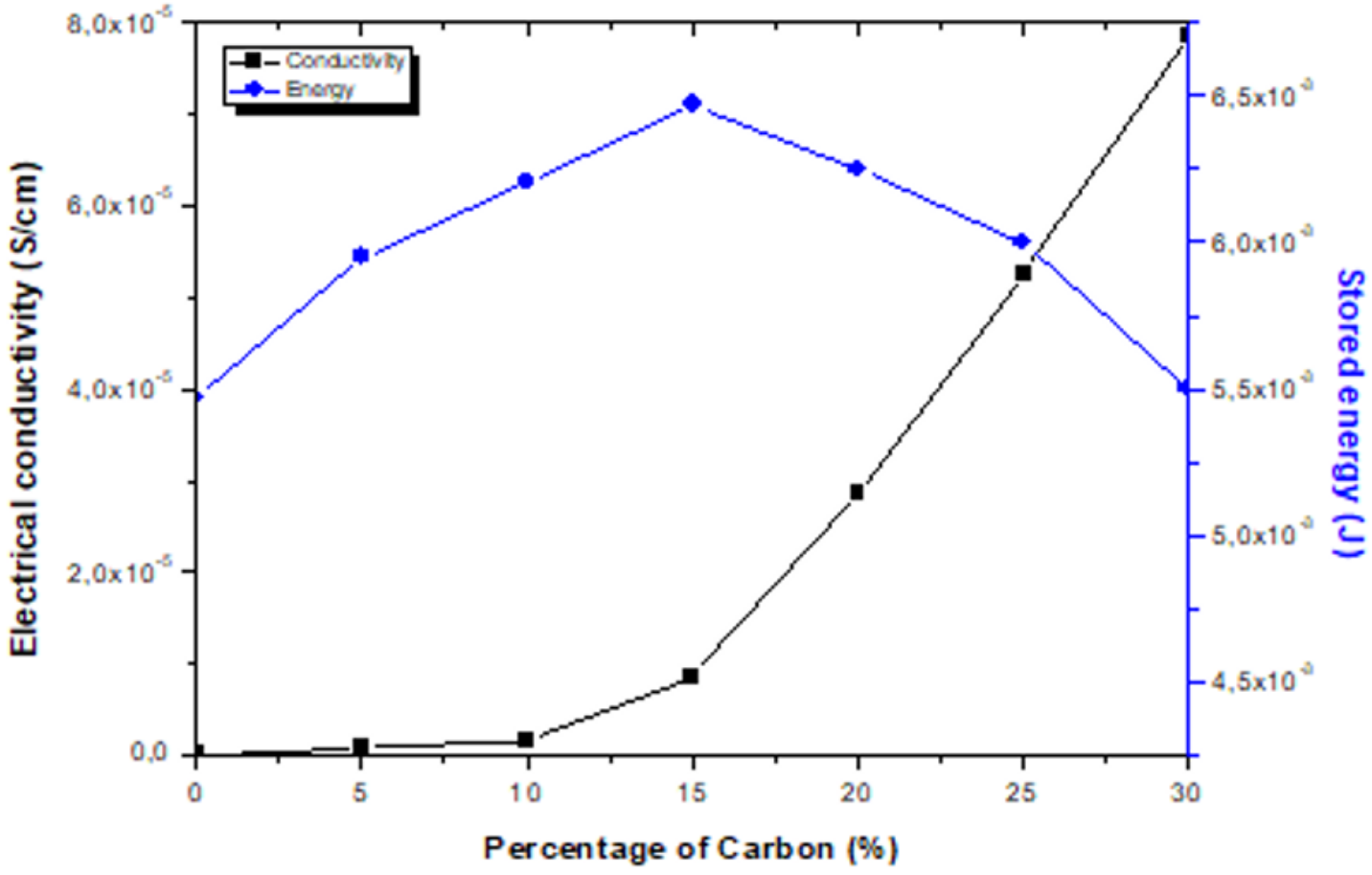

Figure 3

Electrical Conductivity and Stored Energy vs. carbon additions in the LFP/rGO nanocomposite

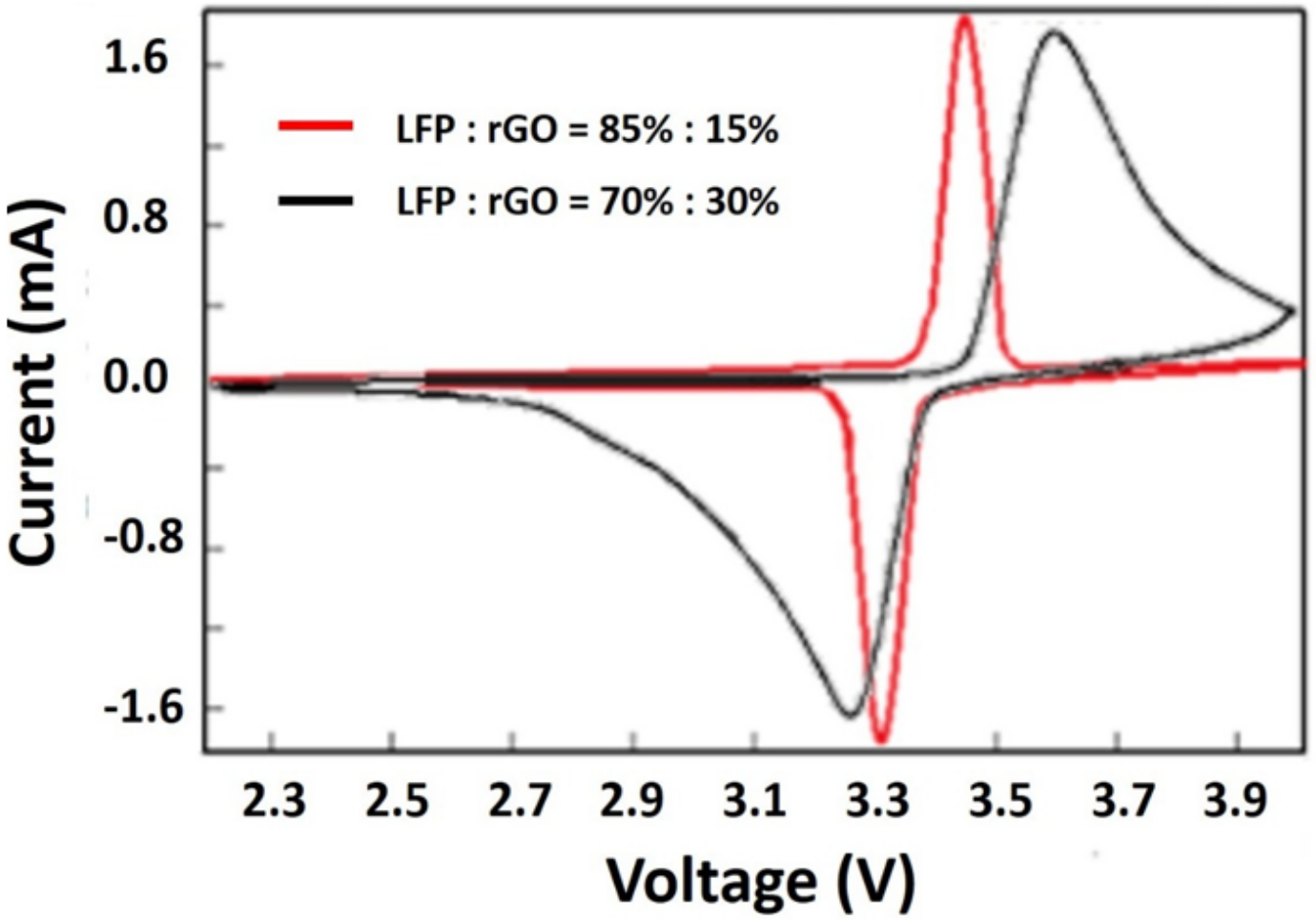

Figure 4

The cyclic voltammetry curves of cathode material sample nanocomposite LiFePO4/rGO at a ratio of 70% - 30% and 85% - 15%

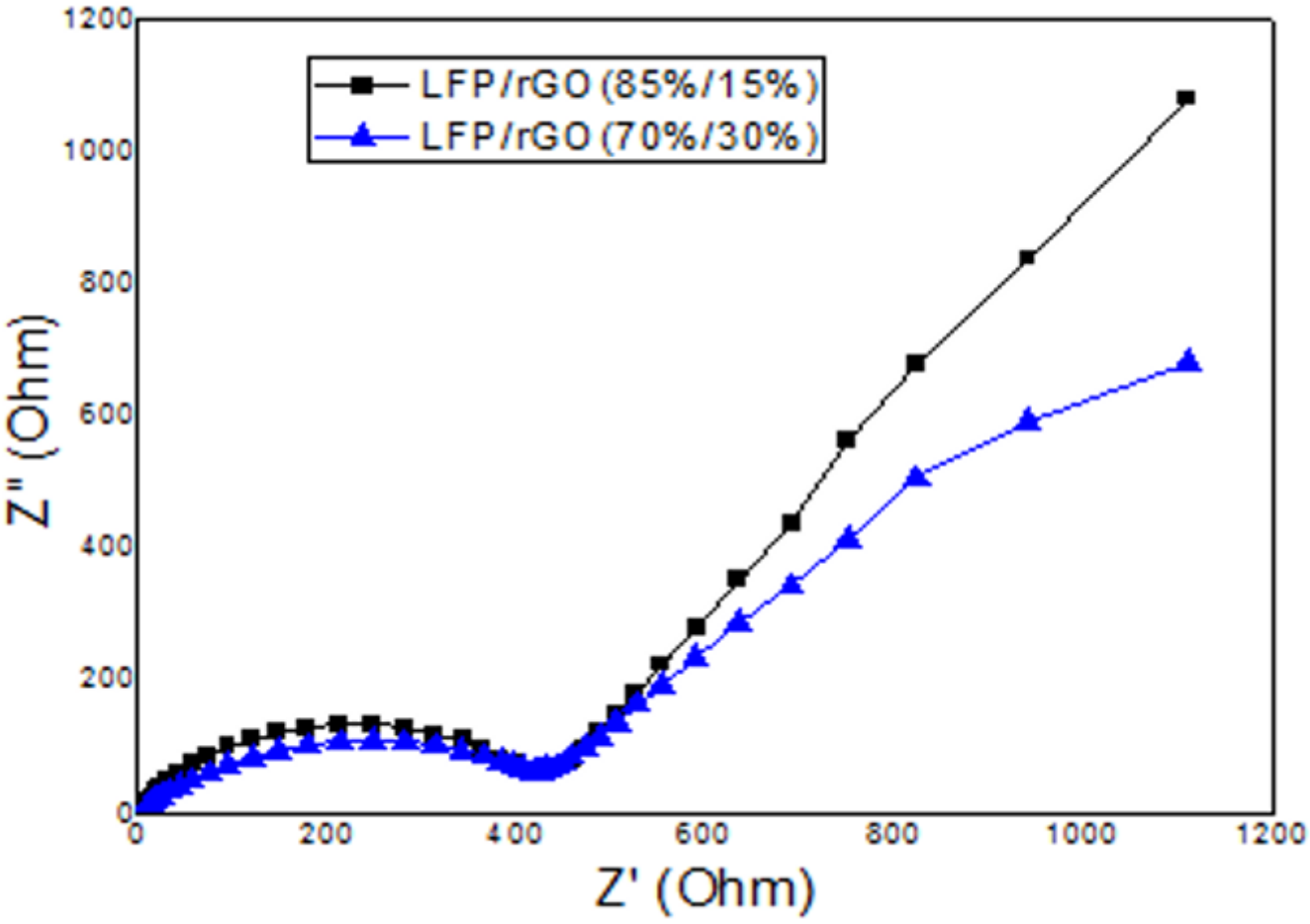

Figure 5

Nyquist plots of nanocomposite LFP/rGO at a ratio of 70% - 30% and 85% - 15%

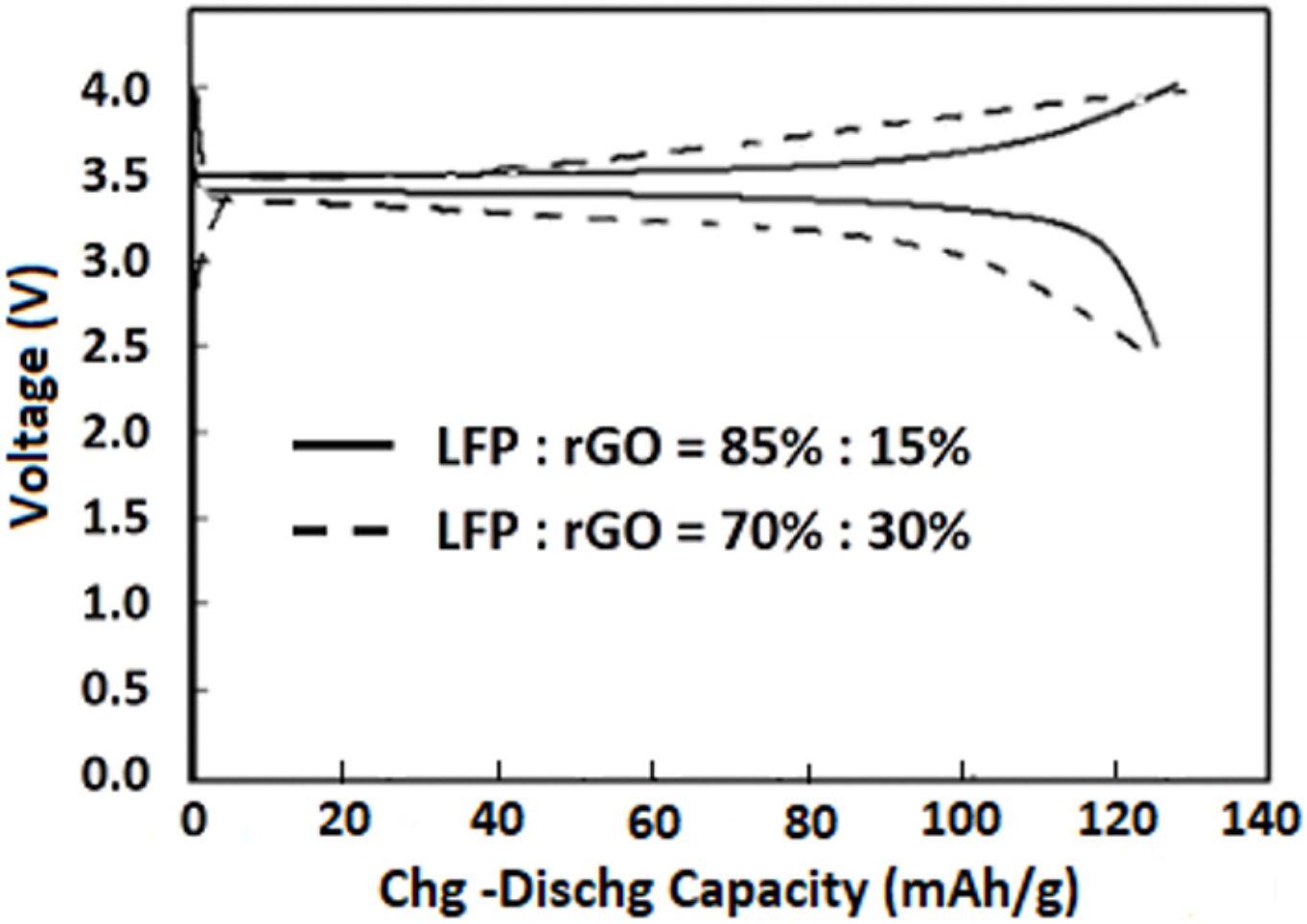

Figure 6

Initial curve of charge and discharge of cathode material nanocomposite LFP/rGO sample at a ratio of 70% - 30% and 85% - 15%